



Contents lists available at [SciVerse ScienceDirect](#)

Catalysis Today

journal homepage: www.elsevier.com/locate/cattod



Transformation of aromatic hydrocarbons over isomorphously substituted UTL: Comparison with large and medium pore zeolites

Naděžda Žilková^a, Mariya Shamzhy^{a,b}, Oleksiy Shvets^b, Jiří Čejka^{a,*}

^a J. Heyrovský Institute of Physical Chemistry, Academy of Sciences of Czech Republic, v.v.i. Dolejškova 3, 182 23 Prague 8, Czech Republic

^b L.V. Piszarzhewskiy Institute of Physical Chemistry, National Academy of Sciences of Ukraine, 31 pr. Nauky, Kyiv 03028, Ukraine

ARTICLE INFO

Article history:

Received 23 July 2012

Received in revised form 10 October 2012

Accepted 12 October 2012

Available online xxx

Keywords:

UTL zeolite

Isomorphous substitution

Toluene alkylation with isopropyl alcohol

Toluene disproportionation

Acidity characterization

ABSTRACT

Isomorphously substituted UTL zeolite with heteroatoms Al, Ga and Fe was synthesized, characterized by X-ray powder diffraction, scanning electron images, nitrogen adsorption isotherms and pyridine adsorption followed by FTIR spectroscopy and tested in disproportionation of toluene, toluene alkylation with isopropyl alcohol and trimethylbenzene disproportionation/isomerization. The catalytic properties of UTL zeolites were compared with those of BEA and MFI zeolites and the observed differences are discussed. Isomorphously substituted (Al, Ga, Fe) UTL zeolites show in most cases lower conversions for the reactions studied but higher selectivities to more valuable products. For toluene disproportionation reaction UTL zeolites shown higher selectivity to xylenes compared with BEA and MFI. In toluene alkylation with isopropyl alcohol no *n*-propyltoluenes are formed over (Ga)UTL or (Fe)UTL while some traces of this undesired product were observed over (Al)UTL. (Al)UTL shows high selectivity to cymenes and *iso*-/*n*-propyltoluene ratio orders of magnitude higher than for MFI. The initial selectivity to xylenes in trimethylbenzene disproportionation/isomerization decreases in the order (Ga)UTL > (Al)UTL \approx BEA \gg MFI and correlates with increasing of acid centres strength, showing that isomorphously substituted extra-large pore zeolites can be enough active and more selective catalysts in some aromatic hydrocarbon transformation reaction.

© 2012 Elsevier B.V. All rights reserved.

1. Introduction

Transformations of aromatic hydrocarbons form the heart of petrochemistry having alkylations of benzene and toluene with ethylene/propylene, disproportionation of toluene to benzene and xylenes, transalkylations of diethylbenzene or di-isopropylbenzene with benzene to provide ethylbenzene or cymene, xylene isomerization, and trimethylbenzene upgrading, as key reactions [1]. Zeolites play dominant role in catalyzing these reactions [2–4] after replacement of aluminium trichloride or solid phosphoric acid [5]. The replacement by zeolites represented a substantial improvement in aromatic large-scale technologies resulting in increasing conversions, selectivities, long-term stabilities together with removal of corrosion and other environmental issues [6].

Zeolites form very important group of industrially relevant adsorbents [7,8] and catalysts [9–11], number of new zeolite structures is continuously increasing and although zeolites are considered as mature catalysts, there exist still many potential applications [12–14]. Mobil Oil introduced several these processes

having ZSM-5 as a key catalyst component. The reactions were carried out in a gas phase [15] and later on alkylation reactions were shifted to a liquid phase using zeolites Beta, MCM-22 or Mordenite as catalysts [16]. In addition to a large potential of zeolites for industrial catalytic reactions, particularly in the area of synthesis of chemical specialties, zeolites serve as model catalysts due to their well-defined structures [17]. In the case of transformations of aromatic hydrocarbons, zeolites exhibit shape-selective properties depending on the size and connectivity of the channel systems. Thus, any new zeolite or its particular morphology is usually tested in these reactions to provide a clear picture about the effect of structure/composition on zeolite activity/selectivity [18].

Recently, zeolite UTL has been synthesized exhibiting for the first time two-dimensional channel system of intersecting extra-large 14- and large 12-rings [19–21]. This zeolite not only represents important achievement in understanding of the synthesis of zeolites but also affords for investigation of the catalytic behaviour of this novel zeolite. Recently, catalytic testing in the *n*-decane hydroisomerization/hydrocracking reaction was performed for UTL, (B)- and (Al)UTL [22–24]. In addition, the structure of UTL zeolite, consisting of layers connected together via D4R, enables post-synthesis hydrolysis leading to separated preserved layers [25] offering further manipulation well-described for MCM-22 family [26].

* Corresponding author.

E-mail address: Jiri.cejka@jh-inst.cas.cz (J. Čejka).

In this contribution, we report on the catalytic behaviour of isomorphously substituted UTL zeolite with Al, Ga, and Fe in the framework. All UTL zeolites were synthesized by direct synthesis, characterized by X-ray powder diffraction, scanning electron microscopy, nitrogen sorption isotherms, and FTIR spectroscopy using pyridine and 2,6-*di-tert*-butyl pyridine as probe molecules. The particular attention was devoted to the investigation of catalytic properties of UTL zeolites in gas-phase toluene disproportionation and toluene alkylation with isopropyl alcohol and trimethylbenzene disproportionation/isomerization. The behaviour of UTL zeolites was related to standard zeolites ZSM-5 (three-dimensional 10-ring channel system) and Beta (three-dimensional 12-ring zeolites).

2. Experimental

2.1. Standard zeolites

Zeolites MFI and BEA were purchased from Zeolyst and used after four-times repeated ion-exchange with 0.5 M solution of ammonium nitrate (100 ml of solution/1 g). After that the zeolites were activated in situ prior to the catalytic experiments to remove the ammonium cations.

2.2. Synthesis of template

Preparation of 7-ethyl-6-azoniaspiro[5.5]undecane hydroxide, used here as structure directing agent, was carried out using a method similar to Ref. [27]. The yield of the product was about 92%. The successful synthesis of the structure-directing agent was confirmed by ^1H NMR spectroscopy after dissolution in [D6] dimethyl sulfoxide.

2.3. Synthesis of UTL zeolites

UTL zeolites were synthesized similarly to Ref. [27] replacing a part of silica source for the required amount of the freshly precipitated gel of relevant heteroatom. Molar compositions of reaction mixtures were 0.782 SiO_2 :0.018 $\text{EO}_{1.5}$:0.4 GeO_2 :0.7 ROH/Br:30 H_2O (E = Al, Ga and Fe). Typically, the source of the respective heteroatom was dissolved (or dispersed in the case Fe) in a water solution of SDA in hydroxide/bromide form. Then, crystalline germanium oxide was added and the mixture was stirred at room temperature for 30 min until its total dissolution. After this, silica (Aerosil 300) was added into the obtained solution and the mixture was stirred at room temperature for another 30 min. Finally, the required amount of concentrated HCl or SDAs solution was added to the above mixture under vigorous stirring to adjust pH of the gel to 12.0 (Al), 11.8 (Fe) and 10.8 (Ga). The pH of this gel was measured at 25 °C with a glass pH electrode in conjunction with a digital pH meter (ECOSCAN pH5). The resulting fluid gel was charged into 25 ml Teflon-lined autoclaves and heated at 175 °C for 20 (Al), 10 (Fe) and 13 (Ga) days under agitation (~25 rpm). Usually, to achieve an appropriate mixing of the reaction mixture, a small Teflon cylinder was inserted into the autoclave. The solid products obtained after preset synthesis times were recovered by filtration, washed out with distilled water and dried overnight at 95 °C. To remove the SDA, the as-synthesized zeolites were calcined in a stream of air at 550 °C for 6 h with a temperature ramp of 1 °C/min.

2.4. Characterization

2.4.1. Chemical analysis

The chemical composition of UTL zeolites was determined by elemental analysis. For this purpose 0.2–0.3 g of zeolite sample was heated at 70 °C with 5–7 ml of 10 M NaOH in a platinum cup.

After total dissolution of zeolite sample, 10–15 ml of concentrated HCl was added until pH became 0.6–0.7 and acid solution was evaporated at 80 °C during 1 h. Under such conditions, Ge evaporated from the solution in the form of GeCl_4 [28], but volatilization of other elements under study is negligible (<3%) [29]. Then to acidized residue, 10–15 ml of concentrated HCl and after 10 min also 50 ml of hot water were added. The precipitate was recovered by filtration on ash-less filter, washed out with 1 M HCl, then with hot water for complete removal of AlCl_3 , GaCl_3 , or FeCl_3 . Precipitated $\text{SiO}_2 \cdot x\text{H}_2\text{O}$ was dried at 90 °C, calcined at 1000 °C until the constant mass and weighed.

For the quantitative determination of Ge, UTL zeolite sample was refluxed with concentrated hydrochloric acid for 1 h, precipitated SiO_2 was recovered by filtration. GeCl_4 was extracted from the filtrate with CCl_4 and quantitatively determined by back-complexation titration as described elsewhere [30].

Ga and Al contents were determined by back-complexation titration using the following procedure. 25.0 ml of 0.05 M EDTA was added to analysed solution and warmed to boiling, then cooled down and neutralized with $\text{NH}_3 \cdot \text{H}_2\text{O}$ (25% solution) until pH = 3. Then 20 ml of acetate buffer solution (pH = 6.0) was added to adjust the pH = 5.5–6.0. This solution was boiling for 5 min to ensure complete complexation of the cations and cooling down to the room temperature. The excess of EDTA was titrated with 0.05 M ZnSO_4 in the presence of xylenol orange until the colour change from yellow to violet.

Analysed solution, containing Fe, was neutralized with 25% solution of $\text{NH}_3 \cdot \text{H}_2\text{O}$ until not vanishing weak feculence appeared. It was dissolved by adding 1–2 drops of 1 M HCl. Then 1 ml of 1 M HCl and 0.5 g of 2-aminoacetic acid were added. Prepared solution was diluted to 50 ml by water and warmed to boiling. Hot solution was titrated with 0.05 M EDTA, using salicylic acid as indicator, until the initial violet colour turned to yellow.

All stages of described method were tested on model mixtures of crystalline GeO_2 , SiO_2 and E_2O_3 (E = Al, Ga, Fe). The experimental error of the determination of each element does not exceed 5 relative %.

X-ray powder diffraction data were obtained on a Bruker AXS D8 ADVANCE diffractometer in the Bragg–Brentano geometry using $\text{Cu K}\alpha$ radiation with a NaI dynamic scintillation detector. To limit the effect of preferential orientation of individual UTL crystals a gentle grinding of the samples to decrease their size and careful packing into the holder was performed.

The shape and size of zeolite crystals were determined by scanning electron microscopy (SEM; JEOL, JSM-5500LV).

The acidity of all zeolite samples was investigated also by the adsorption of pyridine used as probe molecules followed by FTIR spectroscopy [31]. Generally, all samples were activated in a form of self-supporting wafers (ca. 8.3–12.5 mg/cm 3) at 400 °C under vacuum for 2 h prior to the adsorption of probe molecules. The adsorption temperature was 150 °C. The adsorption of probe molecules was investigated on a Nicolet 6700 spectrometer with a resolution of 2 cm $^{-1}$. All measured spectra were recalculated to a “normalized” wafer of 10 mg. For a quantitative characterization of acid sites, the following bands and adsorption coefficients were used: PyH $^+$ band at 1545 cm $^{-1}$, $\epsilon = 1.67 \text{ cm} \mu\text{mol}^{-1}$, PyL bands at 1450–1455 cm $^{-1}$, $\epsilon = 2.22 \text{ cm} \mu\text{mol}^{-1}$ [32].

2.5. Catalytic tests

Toluene disproportionation and toluene alkylation with isopropyl alcohol were studied in the gas phase under atmospheric pressure using a glass fixed-bed reactor with internal diameter of 10 mm. Each catalyst was pressed into the pellets, crushed and sieved to obtain particles with a diameter in the range of 0.50–0.71 mm. Prior to the reaction, a given amount of the catalyst

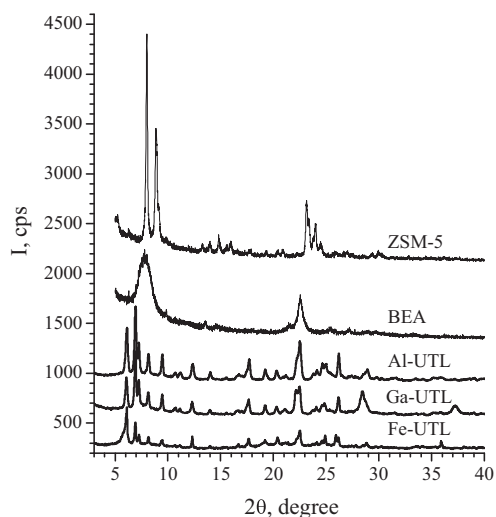


Fig. 1. XRD patterns of all zeolites under study.

was in situ activated at 500 °C for 120 min in a stream of nitrogen (40 ml min⁻¹). After that, the activated catalyst was cooled down to the preset reaction temperature. In the case of toluene disproportionation the reaction temperature was at 450 and 500 °C, WHSV 2 and 20 h⁻¹, and the concentration of toluene in a stream was 18.5 mol%. Toluene alkylation was studied at the reaction temperatures 200 and 250 °C. The WHSV related to toluene was 10 h⁻¹, the concentration of toluene was 18.5 mol%, and toluene to isopropyl alcohol molar ratio was 9.6.

The reaction mixtures were analysed using an on-line gas chromatograph (HP 6890) equipped with an FID detector and a capillary column (DB-5, 50 m × 0.32 mm × 1 μm) in toluene alkylation, while HP-INNOWax column (30 m × 0.32 mm × 0.5 μm) was used for toluene disproportionation studies. The first sample was taken after 15 min of time-on-stream (T-O-S) and the other samples were taken in the interval of 60 min.

Trimethylbenzene disproportionation/isomerization was performed with 300 mg of catalyst (particle size 0.750–0.355 mm) in a down-flow metallic fixed-bed micro-reactor (Microactivity-Reference Unit, PID Eng & Tech, Madrid, Spain) operating at atmospheric pressure. Before the reaction, the catalysts were activated at 490 °C for 90 min in a flow of nitrogen. The reaction was carried out at 450 °C with WHSV 5 h⁻¹ and concentration of mesitylene in nitrogen was 10 mol%. Reaction products were analysed using an on-line gas chromatograph (Agilent 6890 Plus) with flame ionization detector and a high-resolution capillary column (INNOWax).

3. Results and discussion

All prepared isomorphously substituted UTL zeolites were characterized by X-ray powder diffraction, scanning electron microscopy, and nitrogen adsorption isotherms. Pyridine adsorption followed by FTIR spectroscopy was used to evidence the type and concentration of acid sites. X-ray powder diffraction data (Fig. 1, for details see [33]) clearly evidenced high crystallinity and phase purity of all UTL samples under study. This is in a good agreement with adsorption data (Fig. 2) proving a high micropore volume of all samples.

Nitrogen adsorption isotherms of the catalysts under study are depicted in Fig. 2. All UTL zeolites adsorbing large volumes of nitrogen at relatively low pressure, showed a type I isotherm. The presence of a hysteresis loop at $p/p_0 > 0.8$ is probably connected with an interparticle adsorption. Micropore volume of crystalline

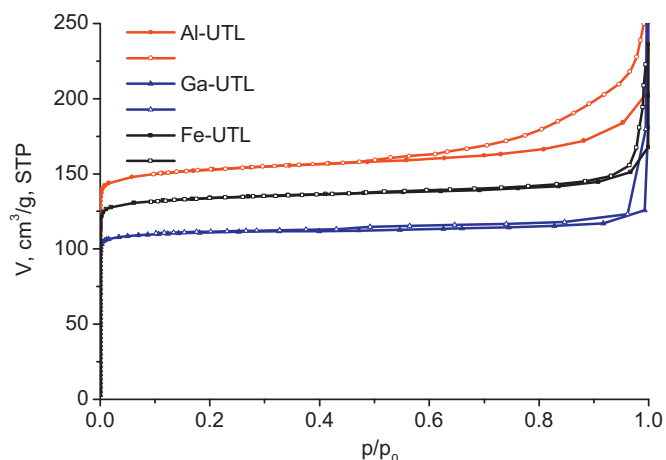


Fig. 2. Nitrogen adsorption isotherms for germanosilicate UTL zeolites containing different isomorphous substituents (adsorption – solid points, desorption – empty points).

zeolite samples was in average 0.19–0.23 cm³/g, while BET areas were in the range 450–600 m²/g. The main reason of subtle changes in the values of BET surface areas and micropore volumes for samples under study is the differences in the degree of their crystallinity. Anyway, micropore volumes about 0.20 cm³/g confirm well-crystalline materials.

All zeolite catalysts exhibit typical rectangular shape of UTL crystals, close to square described in previous reports [19,21]. As can be seen from Fig. 3, the size of the crystals gradually decreases in the range (Fe)UTL > (Ga)UTL > (Al)UTL (Fig. 3 and Table 1). In contrast, size of the crystals of MFI and BEA zeolites is equal or below 1.0 μm, respectively.

Acidic properties of the UTL zeolites, namely the type and concentration of Brønsted and Lewis acid sites, were assessed using adsorption of pyridine followed by FTIR (Fig. 4 and Table 1). FTIR spectra of zeolites exhibit characteristic absorption band at about 3732–3742 cm⁻¹ (attributed to external Si–OH groups) and 3653–3673 cm⁻¹ (attributed to external Ge–OH groups). In addition, Al-containing UTL zeolite exhibits low intensity band at 3610 cm⁻¹ typically assigned to the Brønsted bridging acid sites [31]. Although, we did not observe sharp absorption bands, usually attributed to ≡E–(OH)–Si≡ groups for Ga- and Fe-substituted UTL zeolites, low intensity bands at 3625 cm⁻¹, (Ga)UTL, and 3626 cm⁻¹, (Fe)UTL may evidence the presence of small amount of ≡E–(OH)–Si≡ bridging OH groups. After adsorption of pyridine new absorption bands appeared in the region 1400–1600 cm⁻¹. The absorption band around 1546 cm⁻¹ is due to the interaction of pyridine with Brønsted acid sites while new band around 1450–1455 cm⁻¹ is characteristic of the pyridine adsorbed on Lewis acid sites. The concentration of Brønsted acid centres increased in the range (Fe)UTL < (Ga)UTL ≪ (Al)UTL. This is probably connected with the highest affinity of aluminium for substitution of Si in the framework of UTL in comparison with Fe and Ga.

Catalytic performance of UTL zeolites with Al, Ga and Fe in the framework was confirmed with MFI and BEA zeolites and assessed using toluene disproportionation, toluene alkylation with isopropyl alcohol and trimethylbenzene disproportionation/isomerization. The individual zeolites differ in the size and shape of their crystals and concentrations and types of active sites. Particular difference is between UTL zeolites and BEA and MFI. This is not only in the size of the crystals but also in the accessibility of their channel systems. While zeolites BEA and MFI possess three-dimensional (3D) channel systems being accessible from all crystallographic planes, UTL zeolite has only 2D channel system being accessible from the smallest planes.

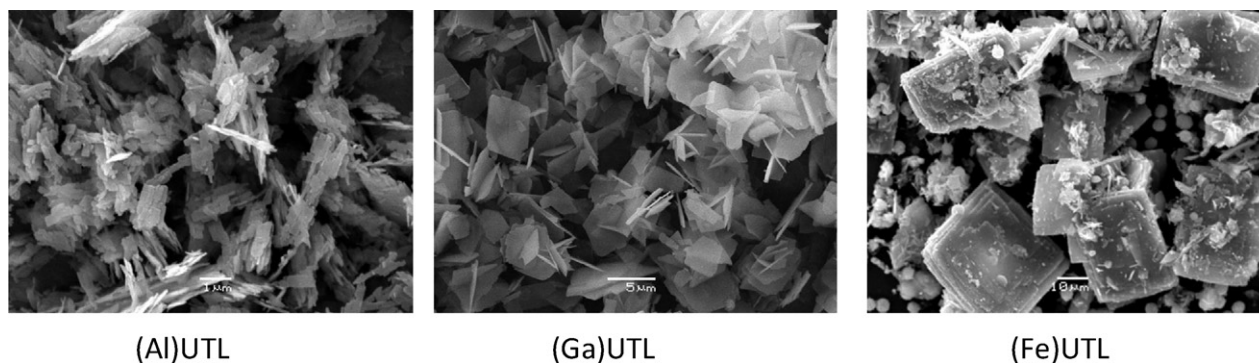


Fig. 3. SEM images of the catalysts under study.

Table 1
Chemical composition, acidic and textural properties of characteristic UTL samples.

Catalyst	Chemical analysis (mol.%)				IR of adsorbed pyridine			V_{micro} (cm ³ /g)	S_{BET} (m ² /g)	Crystal size (μm)
	E ^a	Si	Ge	T(IV)/T(III)	C(Br) (μmol/g)	C(L) (μmol/g)	C(B+L) (μmol/g)			
(Ga)UTL	1.9	74.8	23.3	51.6	14	65	79	0.19	450	5 × 5 × 0.1
(Al)UTL	2.1	72.8	25.1	46.6	69	61	130	0.23	600	2 × 0.5 × 0.1
(Fe)UTL	3.0	74.8	22.2	32.3	9	121	130	0.21	550	25 × 20 × 5
BEA	7.8	92.2	–	11.8	201	380	581	0.18	480	0.3
MFI	2.6	97.4	–	38.1	159	72	231	0.16	305	1.0

^a Al, Ga, Fe.

In the case of toluene disproportionation carried out at 450 °C and WHSV 20 h⁻¹ (Fig. 5), it is clearly seen that zeolite BEA possessing the 3D 12-ring channel system, the smallest crystal size and the highest acid site concentration, exhibits the highest conversion followed by (Al)UTL, MFI, and (Ga)UTL. Although the UTL zeolite has intersecting 14- and 12-ring channels, toluene conversion was higher over zeolite Beta. It indicates that 3D channel system of zeolite Beta with much smaller crystals size enables probably a faster diffusion (also has a higher concentration of acid sites) resulting in a high toluene conversion than the 2D system of larger channels of UTL zeolite. Apparently, a decisive influence on the value of the

conversion has a high concentration of strong acid sites in zeolite BEA as compared with zeolites UTL. In contrast, (Fe)UTL was not active at all. As far as the selectivities are concerned, xylene/benzene molar ratio is between 0.90 and 0.95 for all catalysts under study. This shows that secondary reactions are strongly limited. It should be noted that for (Al) and (Ga)UTL zeolites, the selectivity to *p*-xylene is considerably higher than that for the BEA and MFI zeolites. This is unexpected result, which needs further investigation.

Simultaneous increase in the reaction temperature to 500 °C with a decrease in WHSV results in higher toluene conversions

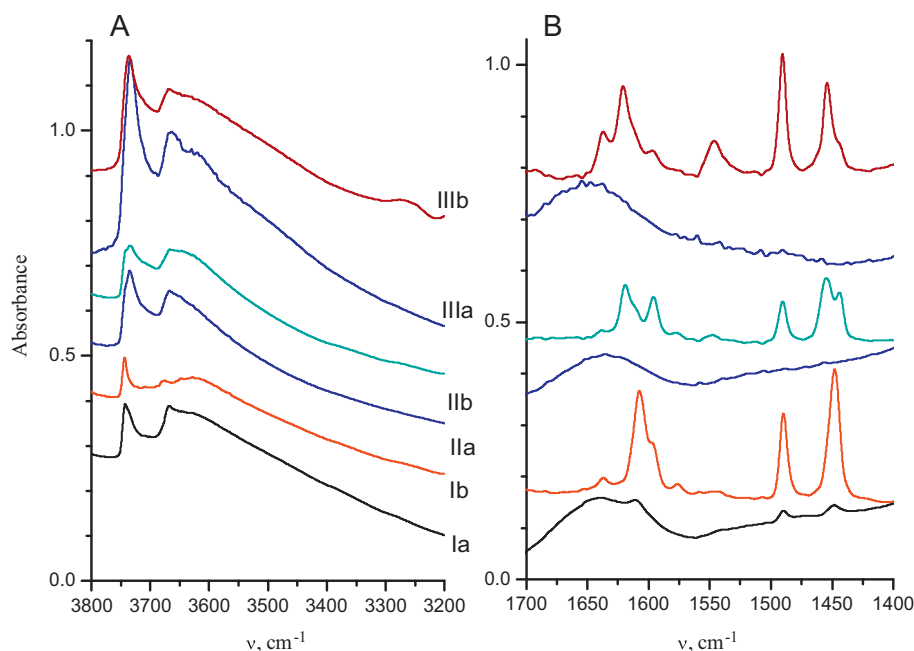


Fig. 4. IR spectra of hydroxyl vibration region of UTL before (a) and after (b) pyridine adsorption (A) and spectra of pyridine after its adsorption (B): (Fe)UTL (I), (Ga)UTL (II), and (Al)UTL (III).

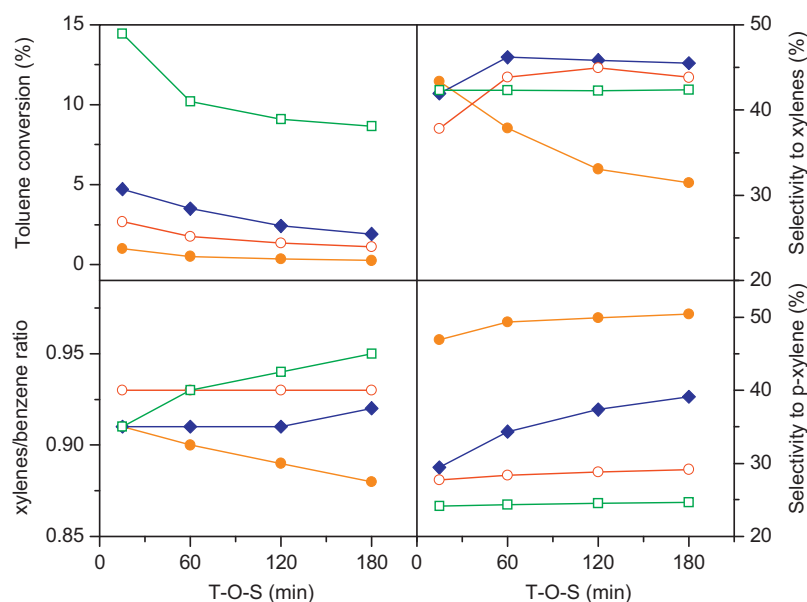


Fig. 5. Time-on-stream dependence of toluene conversion and some selectivities in toluene disproportionation; reaction temperature 450 °C; WHSV 20 h⁻¹; MFI (○), BEA (□), (Ga)UTL (●), and (Al)UTL (◆); selectivity to *p*-xylene in xylene mixture.

of all zeolite catalysts under study. The initial toluene conversion over zeolite BEA is 50% (Fig. 6) but still higher conversions were achieved under the same reaction conditions over zeolite SSZ-33 being around 63% [34]. The increase in toluene conversion is accompanied by decreasing selectivities to xylenes, lower xylene/benzene molar ratios and lower *p*-xylene selectivities. All these effects are due to a substantial increase in the rates of consecutive reactions at the reaction temperature of 500 °C. The rate of consecutive reactions is controlled by the acid strength of active sites of zeolite catalysts as well as by their structure. The highest xylene/benzene molar ratio was obtained over zeolite MFI. Although MFI exhibits the highest acid strength among other zeolites under study, its 10-ring channel systems strongly blocks the formation of bulkier bi-molecular intermediates or transition states. As a result, consecutive reactions of primarily formed

xylenes are limited providing high xylene/benzene molar ratio. In contrast, when comparing isostructural (Ga)UTL and (Al)UTL, we clearly see that with increasing acid strength (Ga < Al) the rate of consecutive reactions increases.

Toluene alkylation with isopropyl alcohol provides significant insight into the role of structure and acidity of zeolites, in particular with respect to novel zeolites. Fig. 7 gives toluene conversions and some selectivities over zeolites studied. In contrast to toluene disproportionation, even (Fe)UTL zeolite is slightly active in toluene alkylation with isopropyl alcohol. It confirms that acid strength required for activation of reactants in alkylation reaction is lower than for disproportionation. It should be noted that molar ratio toluene to isopropyl alcohol 9.6 was applied limiting the toluene conversion to about 10% if only the alkylation reaction will proceed. Zeolite BEA with three-dimensional channel system, the smallest

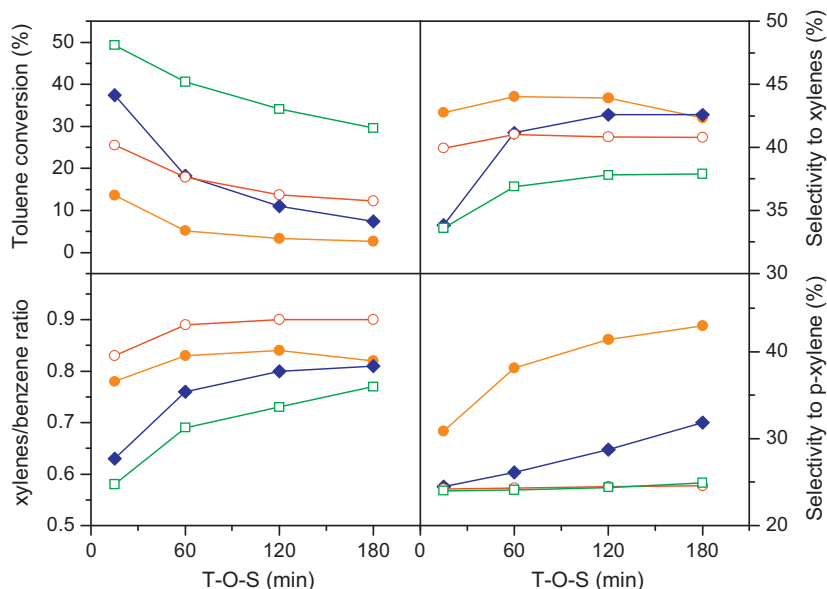


Fig. 6. Time-on-stream dependence of toluene conversion and some selectivities in toluene disproportionation; reaction temperature 500 °C; WHSV 2 h⁻¹; MFI (○), BEA (□), (Ga)UTL (●), and (Al)UTL (◆); selectivity to *p*-xylene in xylene mixture.

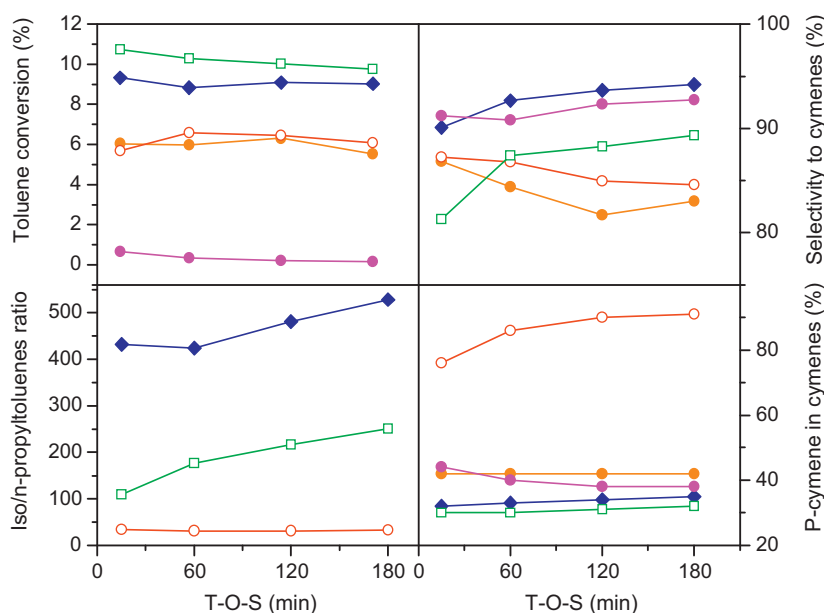


Fig. 7. Time-on-stream dependence of toluene conversion and some selectivities in toluene alkylation with isopropyl alcohol; reaction temperature 200 °C; WHSV 10 h⁻¹; MFI (○), BEA (□), (Fe)UTL (●), (Ga)UTL (●), and (Al)UTL (◆); selectivity to *p*-cymene in cymene mixture.

crystal size, and the highest acid centres concentration, is again more active than (Al)UTL although lower acid strength is needed for this reaction. Fig. 7 clearly shows that with increasing acid strength of acid sites the toluene conversion increases as well reaching about 10% for (Al)UTL (Fe < Ga < Al). Although the conversion decreases in the sequence Al > Ga > Fe, (Al)UTL exhibits simultaneously the highest selectivity to cymenes. One can infer that this is due to a lowest concentration of Lewis acid sites among isomorphously substituted UTL zeolites. No *n*-propyltoluenes are formed over (Ga)UTL or (Fe)UTL while some traces of this undesired product are observed over (Al)UTL. It confirms the importance of strong acid sites for operating this consecutive bimolecular reaction leading to *n*-propyltoluenes. As for the *para*-selectivity, all UTL zeolites show the selectivity to *p*-cymene close to 40% while 10-ring zeolite MFI gives around 90% after 180 min of TOS. This is a clear evidence of product shape selectivity over MFI zeolite in 10-ring channels and crystal size about 1.0 μm. Comparable or even much larger crystals of UTL zeolites do not provide higher *para*-selectivity in their 14- or 12-ring channels.

The increase in the reaction temperature to 250 °C results in lower toluene conversions for practically all zeolite catalysts (except (Ga)UTL) under study. It is explained in terms of the shift of the alkylation/dealkylation equilibrium [6]. Fig. 8 gives toluene conversions and selectivities at 250 °C over zeolites studied. Similarly as at 200 °C, the conversion of toluene increases as follows (Fe)UTL << MFI ≈ (Ga)UTL < (Al)UTL < BEA, showing good correlation with increasing pore size and strength as well as concentration of acid sites. The increase in the reaction temperature substantially changes the selectivity to cymenes: a sharp decrease was observed for MFI while some increase for (Ga) and (Fe)UTL. In the case of MFI zeolite, the decrease in the selectivity to cymenes is due a higher rate of the bimolecular reaction of isopropyltoluene with toluene to *n*-propyltoluene at higher reaction temperatures. Optimum shape of channel intersections in MFI accelerates this bimolecular reaction [6]; with increasing size of channel intersections the rate of this bimolecular reaction substantially decreases.

Similarly as for toluene disproportionation, in the case of trimethylbenzene transformation, carried out at 450 °C and WHSV 5 h⁻¹ (Fig. 9), it is clearly seen that zeolite Beta also exhibits the highest conversion followed by (Al)UTL, MFI, and (Ga)UTL. (Fe)UTL

sample was not active at all. The initial selectivity to xylenes decreases in the order (Ga)UTL > (Al)UTL ≈ BEA ≫ MFI and correlates with increasing acid centres strength, probably because on stronger acid sites take place following xylene disproportionation into toluene, benzene, etc. Decrease in the selectivity to xylene for (Al)UTL sample with increasing T-O-S probably caused by transfer reaction from the outer surface into micropores where the possibility of xylenes conversion is higher than for tetramethylbenzenes. For (Ga)UTL this decrease takes place to a lesser extent. In contrast, the selectivity of the zeolite BEA has remained largely unchanged. Zeolite BEA exhibits the smallest crystals, thus, a high concentration of strong acid sites in channel entrances is probably responsible for constant running of trimethylbenzene disproportionation to xylenes and tetramethylbenzenes. Probably xylene and tetramethylbenzenes molecules formed on the outer surface undergo further transformations with constant rate ratio. The fact that xylene/TeMBS ratio for BEA zeolite was less than 1 shows that tetramethylbenzene molecules are less active on the outer surface compared to xylene. In contrast, for isomorphously substituted extra-large pore zeolites, disproportionation of tetramethylbenzenes is possible in pores, as results, xylene/TeMBS ratio was more than 1.

Figs. 5–9 present time-on-stream dependences of reactant conversions and some selectivities to individual products. The conversions obtained usually differ substantially as the individual catalysts exhibit big differences in their activities (due to different channel systems, types and concentrations of acid sites and size of the channels). To obtain appropriate comparison of the catalysts behaviour in the individual reactions, selectivities to xylenes (cymenes) were plotted against conversion (Fig. 10). In toluene disproportionation (Fig. 10A), toluene conversion over zeolite Beta approaches the thermodynamic values at the reaction temperature 500 °C, followed by (Al)UTL zeolite. This clearly evidences the importance of both the acid site strength as well as the accessibility of active sites in the microporous channel system. Selectivity to xylenes decreases only slightly with increasing toluene conversion, which is mainly due to the limitations of the consecutive reactions from shape-selectivity reasons.

Similar situation is observed for trimethylbenzene disproportionation (Fig. 10B). MFI and (Ga)UTL zeolites exhibit conversions

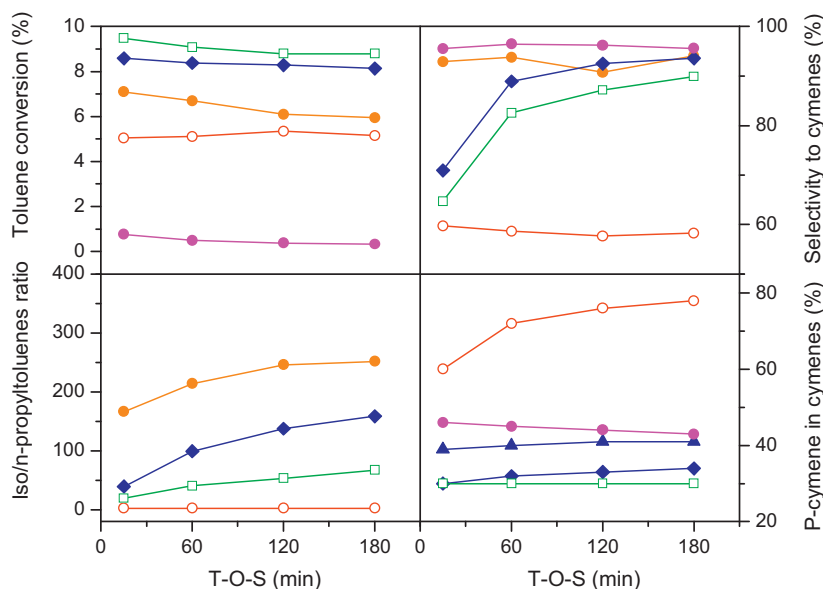


Fig. 8. Time-on-stream dependence of toluene conversion and some selectivities in toluene alkylation with isopropyl alcohol; reaction temperature 250 °C; WHSV 10 h⁻¹; MFI (○), BEA (□), (Fe)UTL (●), (Ga)UTL (●), and (Al)UTL (◆); selectivity to *p*-cymene in cymene mixture.

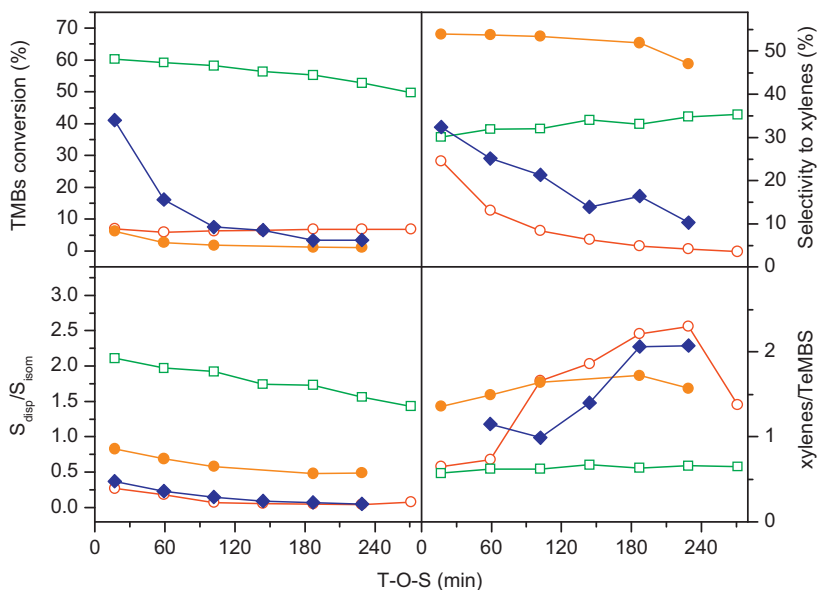


Fig. 9. Time-on-stream dependence of trimethylbenzene conversion and some selectivities in trimethylbenzene disproportionation/isomerization; reaction temperature 450 °C; WHSV 5 h⁻¹; MFI (○), BEA (□), (Ga)UTL (●), and (Al)UTL (◆).

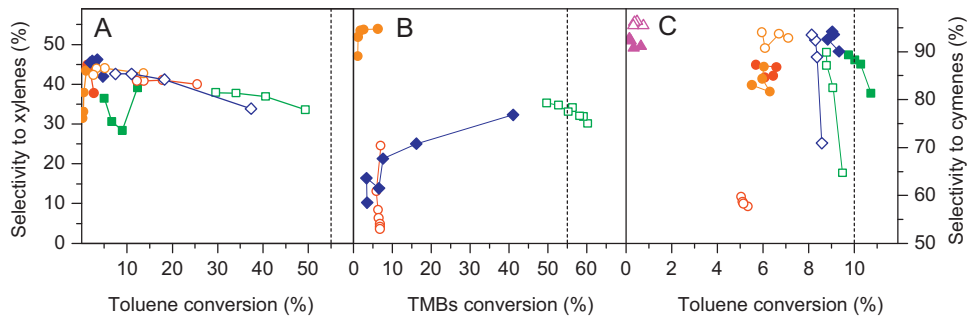


Fig. 10. The dependence of selectivities to xylenes in toluene (A) and trimethylbenzene (B) disproportionation and cymenes in toluene alkylation with isopropyl alcohol (C) on toluene, trimethylbenzene and toluene conversion, respectively. Reaction temperatures: toluene disproportionation 450 °C (full points), 500 °C (empty points); trimethylbenzene disproportionation 450 °C; toluene alkylation 200 °C (full points), 250 °C (empty points); MFI (○), BEA (□), (Ga)UTL (●), and (Al)UTL (◆); thermodynamic conversions for primary reactions (calculated by Aspen Plus) – dotted line.

less than 10%. Lower acid strength of active sites in (Ga)UTL is the main reason for achieving around 50% of selectivity to xylenes. In contrast, zeolite Beta shows again TMB conversions close to thermodynamic values. Slightly higher conversions than thermodynamic limits are due to the consecutive reaction of primary products as well as some dealkylation of TMB (Fig. 10B).

In the case of toluene alkylation (Fig. 10C), toluene conversions over (Al)UTL and BEA are close to thermodynamic values and selectivities to cymenes (primary products) are usually higher than 80%. The exceptions are at 250 °C for zeolites (Al)UTL and BEA (short T-O-S values) when the toluene conversion is also influenced by toluene disproportionation and secondary alkylation providing di-isopropyltoluenes. Concentrations of by-products decreased significantly within the first 60 min of the reaction (cf. Figs. 8 and 10). In the case of MFI zeolite, low selectivity to cymenes at 250 °C is the result of the consecutive bimolecular reaction between cymenes and toluene providing undesired *n*-propyltoluene. The rate of this reaction is significantly enhanced at 250 °C and proceeds particularly in the channel system of MFI zeolite [6].

4. Conclusions

Isomorphously substituted UTL zeolites were synthesized by direct method, characterized by X-ray powder diffraction, scanning electron images, nitrogen adsorption isotherms and pyridine adsorption followed by FTIR spectroscopy to evidence the type and concentration of acid sites. In addition, they were tested as catalysts in toluene disproportionation, toluene alkylation with isopropyl alcohol and trimethylbenzene disproportionation/isomerization reaction. The catalytic properties of UTL zeolites were compared with those of BEA and MFI zeolites and the observed differences are discussed. Isomorphously substituted (Al, Ga, Fe) UTL zeolites show in most cases lower conversions for the reactions studied, most probably due to a lower concentration of strong acid sites.

Comparison of selectivities to primary reaction products at different conversion levels evidences the key role of the channel system of zeolites under study. With increasing pore size, higher conversions as well as selectivities were obtained, indicating the dominating role of zeolites BEA and (Al)UTL. For the same channel system (zeolite UTL), concentration and strength of acid sites are important as well showing the order Al > Ga > Fe.

In toluene alkylation with isopropyl alcohol no *n*-propyltoluenes are formed over (Ga)UTL or (Fe)UTL while some traces of this undesired product were observed over (Al)UTL. However, *iso*-/*n*-propyltoluene ratio obtained for (Al)UTL is two orders of magnitude higher than for MFI, evidencing again the critical role of the channel intersection architecture for the formation of *n*-propyltoluenes. (Al)UTL zeolite also exhibits high selectivity to cymenes.

BEA zeolite exhibits the highest conversion of trimethylbenzene in their disproportionation while a higher acid strength of (Al)UTL is decisive for higher conversion than for (Ga)UTL. These results

indicate that isomorphously substituted extra-large pore zeolites can be sufficiently active and even more selective catalysts for some aromatic hydrocarbon transformations.

Acknowledgements

The authors thank the Czech Science Foundation (Project No. P106/12/0189) for financial support. J.Č. appreciates very much the Micromeritics Grant Program supporting his research activities.

References

- [1] W.W. Kaeding, G.C. Barile, M.M. Wu, *Catalysis Reviews: Science and Engineering* 26 (1984) 597.
- [2] T.C. Tsai, S.B. Liu, I. Wang, *Applied Catalysis A* 181 (1999) 355.
- [3] S. Rabiou, S. Al-Khattaf, *Industrial and Engineering Chemistry Research* 47 (2008) 39.
- [4] S. Melson, F. Schüth, *Journal of Catalysis* 170 (1997) 46.
- [5] C. Perego, P. Ingallina, *Catalysis Today* 73 (2002) 3.
- [6] J. Čejka, B. Wichterlová, *Catalysis Reviews: Science and Engineering* 44 (2002) 375.
- [7] S. Choi, McML. Gray, C.W. Jones, *ChemSusChem* 4 (2011) 628.
- [8] A. Pulido, P. Nachtigall, A. Zukal, I. Dominguez, J. Čejka, *Journal of Physical Chemistry B* 113 (2009) 2928.
- [9] T.F. Degnan Jr., *Topics in Catalysis* 13 (4) (2000) 349.
- [10] M. Bejblová, D. Procházková, J. Čejka, *ChemSusChem* 2 (2009) 486.
- [11] J. Čejka, G. Centi, J. Perez-Pariente, W.J. Roth, *Catalysis Today* 179 (2012) 2.
- [12] C. Martínez, A. Corma, *Coordination Chemistry Reviews* 255 (2011) 1558.
- [13] R.E. Morris, *Topics in Catalysis* 53 (2010) 1291.
- [14] D. Kubička, M. Kangas, N. Kumar, M. Tiitta, M. Lindblad, D. Murzin, *Topics in Catalysis* 53 (2010) 1438.
- [15] G.R. Meima, *CATTECH* 3 (1998) 5.
- [16] P. Prokešová, N. Žilková, S. Mintova, T. Bein, J. Čejka, *Applied Catalysis A* 281 (2005) 85.
- [17] A. Corma, *Chemical Reviews* 95 (1995) 559.
- [18] K. Na, M. Choi, W. Park, Y. Sakamoto, O. Terasaki, R. Ryoo, *Journal of the American Ceramic Society* 132 (2010) 4169.
- [19] A.M.J.D. Corma, D. Boughay, *Chemical Communications* (2004) 1356.
- [20] J.L. Pailaud, B. Harbuzaru, J. Patarin, N. Bats, *Science* 304 (2004) 990.
- [21] O.V. Shvets, M.V. Shamzhy, P.S. Yaremov, Z. Musilová, D. Procházková, J. Čejka, *Chemistry of Materials* 23 (2011) 2573.
- [22] N. Kasian, T.I. Koranyi, G. Vanbutsele, K. Houthoofd, J.A. Martens, C.E.A. Kirschhock, *Topics in Catalysis* 53 (2010) 1374.
- [23] N. Kasian, G. Vanbutsele, K. Houthoofd, T.I. Koranyi, J.A. Martens, C.E.A. Kirschhock, *Catalysis Science and Technology* 1 (2011) 246.
- [24] N. Kasian, E. Verheyen, G. Vanbutsele, K. Houthoofd, T.I. Koranyi, J.A. Martens, C.E.A. Kirschhock, *Microporous and Mesoporous Materials* (2012), <http://dx.doi.org/10.1016/j.micromeso.2012.07.017>
- [25] W.J. Roth, O.V. Shvets, M. Shamzhy, P. Chlubná, M. Kubů, P. Nachtigall, J. Čejka, *Journal of the American Chemical Society* 133 (2011) 6130.
- [26] W.J. Roth, J. Čejka, *Catalysis Science and Technology* 1 (2011) 43.
- [27] O.V. Shvets, N. Kasian, A. Zukal, J. Pinkas, J. Čejka, *Chemistry of Materials* 22 (2010) 3482.
- [28] H.B. Rayner, *Analytical Chemistry* 35 (1963) 1097.
- [29] S. Wakamatsu, *Japan Analyst* 7 (1958) 309.
- [30] H.H. Krause, O.H. Johnson, *Analytical Chemistry* 25 (1953) 134.
- [31] Z. Musilová-Pavlačzková, S.I. Zones, J. Čejka, *Topics in Catalysis* 53 (2010) 273.
- [32] C.A. Emeis, *Journal of Catalysis* 141 (1993) 347.
- [33] M. Shamzhy, O.V. Shvets, M.V. Opanasenko, P.S. Yaremov, L.G. Sarkisyan, P. Chlubna, A. Zukal, V.R. Marthala, M. Hartmann, J. Čejka, *Journal of Materials Chemistry* 22 (2012) 15793.
- [34] S. Al-Khattaf, Z. Musilová-Pavlačzková, M.A. Ali, J. Čejka, *Topics in Catalysis* 52 (2009) 140.